catalysts

MDPI

Article

Continuous-Flow Hydrogenation of Methyl Levulinate Promoted by Zr-Based Mesoporous Materials

Noelia Lázaro [1], Ana Franco [1], Weiyi Ouyang [1], Alina M. Balu [1], Antonio A. Romero [1], Rafael Luque [1,2,*] and Antonio Pineda [1,*]

[1] Departamento de Química Orgánica Universidad de Córdoba, Edificio Marie Curie (C 3), Campus de Rabanales, Ctra Nnal IV-A, Km 396, E14014 Cordoba, Spain; bt2laron@uco.es (N.L.); b12frloa@uco.es (A.F.); qo2ououw@uco.es (W.O.); qo2balua@uco.es (A.M.B.); qo1rorea@uco.es (A.A.R.)

[2] Peoples Friendship University of Russia (RUDN University), 6 Miklukho-Maklaya str., 117198 Moscow, Russia

* Correspondence: q62alsor@uco.es (R.L.); q82pipia@uco.es (A.P.); Tel.: +34-957-211-050 (R.L.); +34-957-218-623 (A.P.)

Received: 3 December 2018; Accepted: 2 January 2019; Published: 2 February 2019

Abstract: Several Zr-based materials, including ZrO_2 and Zr-SBA-15, with different silicon/zirconium molar ratios, and ZrO_2/Si-SBA-15 (where SBA-15 stands for Santa Barbara Amorphous material no. 15), have been prepared as hydrogenation catalysts. The materials were characterized using different characterization techniques including X-ray diffraction (XRD), N_2 porosimetry, scanning electron microscopy (SEM/EDX), diffuse reflectance infrared Fourier transform spectroscopy (DRIFT) of pyridine adsorption and the pulsed chromatographic method using pyridine and 2,6-dimethylpyridine as probe molecules, mainly, have been employed for the characterization of the structural, textural, and acidic properties of the synthesized materials, respectively. The catalysts have been evaluated in the hydrogenation reaction of methyl levulinate using 2-propanol as hydrogen donor solvent. The reaction conditions were investigated and stablished at 30 bar system pressure with a reaction temperature of 200 °C using around 0.1 g of catalyst and a flow rate of 0.2 mL/min flow rate of a 0.3 M methyl levulinate solution in 2-propanol. All catalysts employed in this work exhibited good catalytic activities under the investigated conditions, with conversion values in the 15–89% range and, especially, selectivity to ϒ-valerolactone in the range of 76–100% (after one hour time on stream). The highest methyl levulinate conversion and selectivity was achieved by ZrO_2/Si-SBA-15 which can be explained by the higher dispersion of ZrO_2 particles together with a highest accessibility of the Zr sites as compared with other materials such as Zr-SBA-15, also investigated in this work.

Keywords: SBA-15; zirconium; methyl levulinate; ϒ-valerolactone; flow chemistry

1. Introduction

The continuous growing demand on fuel and chemicals, which traditionally have been obtained from petroleum, together with environmental and political factors, have promoted research on alternative and renewable raw materials. In this regard, lignocellulosic biomass constitutes and important renewable carbon source due to its worldwide availability and low price [1–4]. Such lignocellulosic biomass, whose main constituents are cellulose, lignin, and hemicellulose, through different chemical transformations can be transformed into valuable chemicals with different applications such as food additives, polymers, and fuels or fuels additives. Among such chemicals γ-Valerolactone (GVL) is an important chemical easily obtained lignocellulosic biomass, specifically, from the cellulose and hemicellulose fractions. Thus, GVL is an important chemical with many

applications such as sustainable green solvent as well as being precursor of many important chemicals used as intermediates for the production of fuels such as pentanoic or valeric acid, polymers, and fuel additives [3].

The formation of GVL has been reported using homogeneous as well as heterogenous catalysts. Among the homogenous catalysts, Ru-based, including $Ru(acac)_3$ [5] and $RuCl_2(PPh_3)$ [6] compounds are predominantly used for the synthesis of GVL from different substrates such as levulinic acid [5] and glucose [7] among others. Alternatively, the use of solid catalysts entails several advantages such as easy handling and recyclability in addition to the benefits related with the environment. Among the heterogeneous catalyst used to produce GVL via hydrogenation, ruthenium catalysts, mainly Ru/C [8–10] have been the most widely among other noble metals typically used as hydrogenation catalysts including Pt [11] and Pd [12] or bimetallic combinations of these metals with others. Most of these approaches for the synthesis of GVL via hydrogenation are based on the use of molecular hydrogen whose use give rise to several disadvantages such as the low solubility of hydrogen in some solvents or the safety risks that involves the employment of high hydrogen pressures [13]. Alternatively, the use of organic molecules, including, mainly, alcohols and formic acid able to provide the reaction medium with hydrogen through the catalytic transfer hydrogenation (CTH) process. Such approach has been employed in reactions related with biomass valorization process such as the furfural hydrogenation or the conversion of levulinate esters into GVL. The previously mentioned CTH process can be favored by Lewis acid sites including those generated by isomorphic substitution of silicon by metals such as Sn, Zr and Ti in zeolites [14]. Alcohols are the solvents most wide used as hydrogen donor due to their low price, green credentials, and safety in their use. There are some factors that affect the alcohol hydrogen donor efficiency, for instance, secondary alcohols are more capable to transfer hydrogen than a primary alcohol, in addition the alcohol chain length is an important factor, thus, as longer is that chain more favored is the hydrogen transference to the substrate. Such CTH process may take place through different mechanisms that is going to depend on the catalytic species involved in the reaction: homogeneous vs. heterogeneous catalysts or which acid-base or metal catalysts are used for the reaction [13]. In this sense, Zr-based materials represent an efficient and cheap alternative to noble metals leading to high GVL yield comparable to that achieved by more expensive metals such as ruthenium and palladium among others [15,16].

Zirconium loaded materials as well as bulk zirconia are materials widely used in catalysis. Thus, our research group already reported the isomorphic substitution of silicon by zirconium in an SBA-15 framework leading to materials with highly active Lewis acid sites very active in Friedel-Crafts alkylation [17]. Similar approach has been reported for zeolites, where the replacing of aluminum by zirconium give as result a zeolite with enhanced acidic properties and resistant to aqueous environments [18]. In addition, ZrO_2 either supported or bulk owns interesting catalytic features, in addition to its ability of promoting CTH processes, including the combination of both acid and basic properties that allow its participation in cascade processes such as the dehydration of sugars into 5-hydroxymethylfurfural (HMF) [19] or many other applications related with biomass valorization where the water tolerance plays an important role [20,21].

In addition, continuous-flow reactors offer several advantages as compared with traditional batch reactors such the easier scaling up of the reaction conditions, possibility of testing the catalyst along large periods of time on stream in addition other advantages already reported such the high productivity, lower energy consumption, avoids the separation In this sense, continuous-flow processes may offer an attractive option for biomass valorization and the study of the catalysts under certain conditions that may occur including presence of water and moderate temperature and pressure. Moreover, our research group has demonstrated in previous studies the continuous-flow approach is successful alternative for the conversion of biomass derivatives into added value chemicals in biomass valorization processes such as the hydrogenation of furfural [22] or the production of GVL [23,24] that will be also addressed in this work. In addition to these applications, various other reactions have been reported including the continuous hydrogenation of cinammaldehyde over Pt/SiO_2 catalyst coated

tube [25], alkynol semihydrogenation over Pd/ZnO [26] and the continuous gas phase hydrogenation of CO_2 into methanol by CuO/ZnO/ZrO_2 systems [27].

In this work we report the preparation of different Zr-based materials including different phases of ZrO_2, Zr-SBA-15 materials with different Si/Zr ratio prepared by direct synthesis and, finally, ZrO_2 supported on Si-SBA-15 synthesized by wet impregnation with the same loading as the Zr-SBA-15 material with the highest zirconium content, this a 10 wt % metal loading. The different aspects related with their physicochemical properties and the influence of these in the hydrogenation of methyl levulinate under continuous-flow conditions. In addition, different parameters such as flow, temperature and pressure will be optimized.

2. Results and Discussion

The textural properties of the Zr-based materials measured by nitrogen adsorption/desorption measurements are shown in Table 1. As expected, SBA-15 materials own high specific surface while ZrO_2 exhibited lower surface, more specifically the material ZrO_2(m) which showed the lowest surface area (36 m^2/g). The pore diameter measured for mesoporous materials was around 6.0 nm similar to that found for the material ZrO_2(m+c). By contrast, the pore size of the monoclinic zirconium oxide was much higher, so much that this material can be considered more macroporous than mesoporous. Regarding with the pore volume, as well as it happened for the specific surface, this was found higher in the SBA-15 mesoporous materials with a noticeable decrease after the incorporation of ZrO_2 due to the pore blockage by metal oxide particle in a high loading around 10 wt % and the formation ink bottle shaped pores [28].

Table 1. Textural properties of the different Zr-based materials synthesized in this work.

Material	S_{BET} (m^2/g)	V_{BJH} (cm^3/g)	V_{meso} (cm^3/g)	D_{BJH} (nm)
Zr-SBA-15(20)	651	0.79	0.72	6.1
Zr-SBA-15(10)	832	0.95	0.60	5.7
ZrO_2(m)	36	0.28	0.16	26.3
ZrO_2(m+c)	104	0.22	0.15	7.3
ZrO_2/Si-SBA-15	453	0.62	0.56	6.0

The SBA-15 materials showed isotherm plots type IV distinctive for ordered hexagonal SBA-15 materials with a hysteresis loop in a P/Po range between 0.5 and 0.8. The isotherm plot for sample loaded with Pt present a certain deterioration degree as compared with the parent material. The isotherm plots for all the synthesized materials can be found in the Supplementary Materials, Figure S1.

Low angle XRD diffractograms (Figure S2) confirmed the hexagonal arrangement characteristic for SBA-15 materials, showing peaks that can be indexed to diffraction planes 100, 110 and 200, typical for the spatial group P6mm, while this arrangement cannot be observed for the zirconium oxide materials. In addition, the wide-angle XRD of SBA-15 zirconium silicates confirmed the amorphous nature of these materials. The crystallinity of the zirconium oxides samples was evaluated using wide-angle XRD at 2θ between 10° and 80°. The different phases either monoclinic or the mixture of both monoclinic and cubic present in the zirconium oxide materials can be observed on Figure 1.

While the sample ZrO_2(m) shows the characteristics diffraction lines that can be indexed with zirconium oxide in the monoclinic phase, ZrO_2(m+c) presents a mixture of diffraction lines corresponding with both monoclinic and cubic phases. The phases ratio was also measured for the material ZrO_2(m+c), where it was found that approximately the 55% is corresponding with the cubic phase and 45% with the monoclinic phase. The particle size calculated using the Scherrer equation for ZrO_2(m) was 11.6 nm quite similar to that one calculated for ZrO_2(m+c) whose value was 12.1. In the case of the material $ZrO_2$10%/Si-SBA-15, despite of the high Zr loading, any diffraction line

could not be detected as consequence of the high dispersion and small particle size of zirconium on the Si-SBA-15 support.

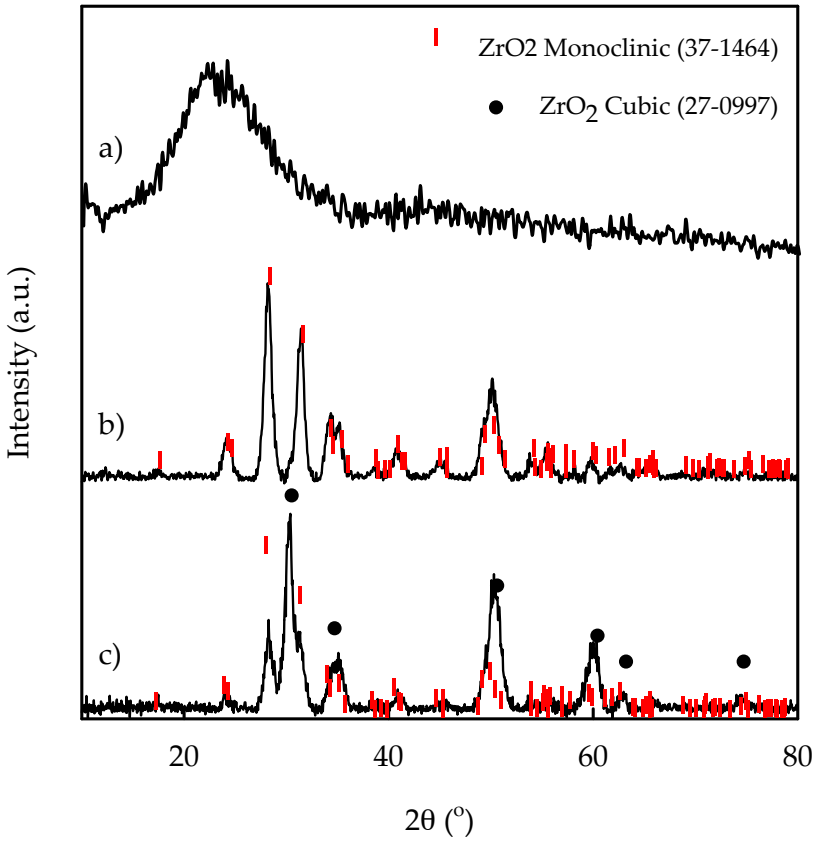

Figure 1. Wide-angle X-ray diffractograms of the synthesized ZrO_2 materials: (**a**) ZrO_2/Si-SBA 15, (**b**) ZrO_2(m) and (**c**) ZrO_2(m+c).

The surface acid properties in the zirconium loaded materials were evaluated by the chromatographic pulse method as well as by DRIFT of pyridine adsorbed. The acidity is going to be an interesting parameter to be evaluated, especially to discern the effect on the selectivity towards GVL. As it can be observed on Table 2, the incorporation of Zr in the SBA-15 framework entails and increase in total acidity, with the highest acidity value found for Zr-SBA-15(10), related with the larger zirconium loading. The material ZrO_2/Si-SBA 15 synthesized by impregnation owns higher both Lewis and Brönsted acidity, which is relate to a better accessibility of the active sites by probe molecules. This nonlinear increase in acidity is produced in Bronsted acidity while Lewis acidity remained unaltered. As expected, in the case of the bulk zirconium oxides these materials showed, mainly, Lewis acid properties together with a negligible amount of Brönsted acid sites.

Table 2. Surface acid properties of the investigated using the chromatographic pulse method.

Catalyst	Si/Zr Molar Ratio *	Total Acidity (μmol Py/g)	Brönsted Acidity (μmol DMPy/g)	Lewis Acidity (μmol/g)	B/L
Zr-SBA-15(20)	26.4	149	25	124	0.2
Zr-SBA-15(10)	12.7	223	101	122	0.8
ZrO_2(m)	-	112	<5	112	<0.1
ZrO_2(m+c)	-	149	<5	149	<0.1
$ZrO_2$10%/Si-SBA-15	12.7	271	120	151	0.8

* Determined by SEM-EDS.

The surface acid properties were measured by pyridine adsorption DRIFT for the material Zr-SBA-15(10) shows a continuous decrease in the interaction strength between pyridine moieties and Brönsted as well as Lewis acid sites with temperature (Figure 2). The characteristics bands for Brönsted and Lewis acid sites at 1550 cm^{-1} and 1442 cm^{-1}, respectively, are distinguishable even at the highest temperature measured, 300 °C. Noticeably, for the SBA-15 materials whose framework has been modified with zirconium, Brönsted acidity remains almost unaltered along the experiment, indicative of the strength of such acid sites.

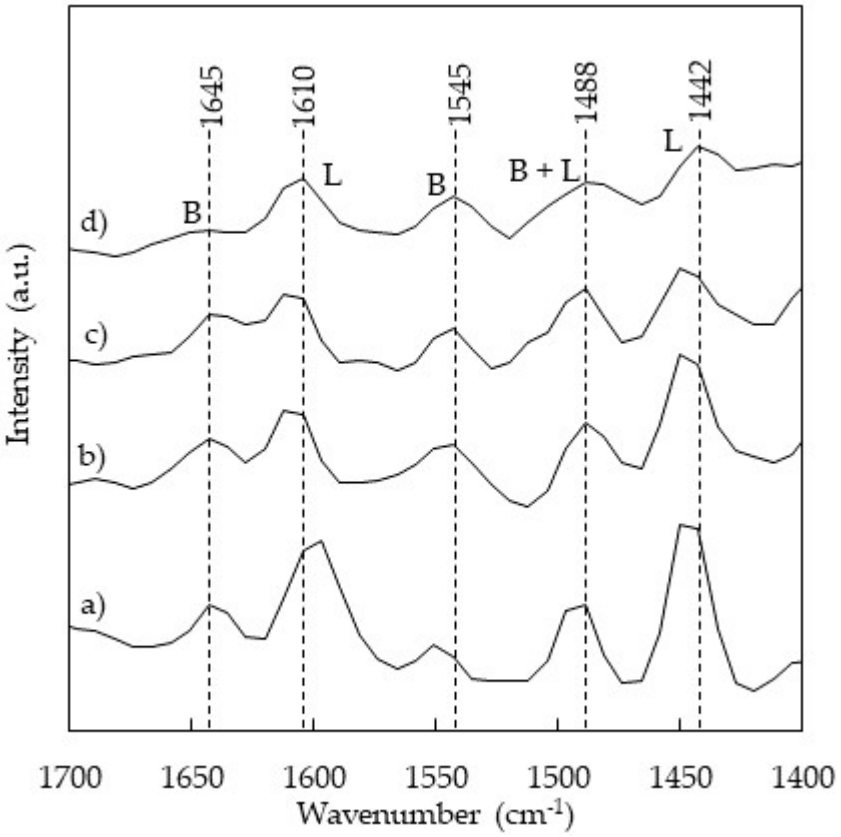

Figure 2. DRIFT spectra of pyridine adsorption on Zr-SBA-15(10) acquired at: (**a**) 100 °C, (**b**) 150 °C, (**c**) 200 °C, (**d**) 300 °C.

The catalytic activity of the Zr-based materials was evaluated in the conversion of methyl levulinate (ML) into ϒ-valerolactone using 2-propanol as H-donor solvent in a liquid-phase continuous-flow reactor (Scheme 1). In general, all the catalysts investigated showed activity in the transformation of ML into GVL. The optimum conditions were stablished for a ML concentration of 0.3 M in 2-propanol with a flow of 2 mL·min^{-1} at 200 °C temperature and the pressure was fixed at 30 bars, according to previously explored reaction conditions by our research group [23]. The first sample was withdrawn after 60 min once the steady state was achieved. The hydrogen donor solvent selected was 2-propanol that as compared with other secondary alcohols such as methanol and ethanol because of its better performance and selectivity as a previous publication of our group shows [23], that is due to the lower reduction potential of 2-propanol as compared with ethanol and methanol [29].

The results for the catalytic screening of the zirconium catalysts are shown in Figure 3. Firstly, regarding with the conversion it can be observed two different performances, while the SBA-15 materials containing Zr in their framework showed conversions below 50 mol.%, a quantitative conversion of ML for ZrO_2 materials in both phases and supported ZrO_2 on SBA-15 silicates was achieved. Remarkably, the conversion for the zirconia catalyst in the monoclinic phase deactivates continuously after the first 30 min of reaction. This deactivation may be caused by the coke deposition

over the small surface of the catalyst. The results for the selectivity towards GVL for the different catalysts investigated reveals, as it happened for the conversion, a smaller selectivity for the Zr-SBA-15 materials, while the highest selectivity to GVL was achieved by both zirconium oxides studied. The decrease in selectivity for the SBA-15 zirconium silicates it is explained by the Brönsted acidity of these materials that favors the transesterification of ML to isopropyl levulinate, the secondary product detected for these catalysts as well as for the supported ZrO_2 on Si-SBA-15.

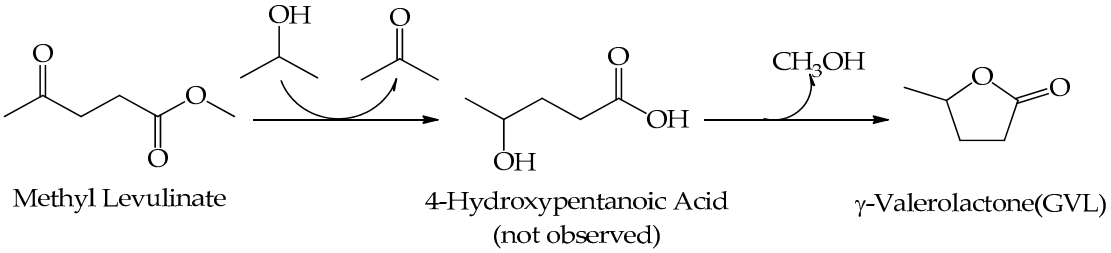

Scheme 1. Methyl levulinate hydrogenation to GVL by Zr-based catalysts using 2-propanol as hydrogen donor solvent. Reproduced from Ref. [30] with permission from The Royal Society of Chemistry [30].

The differences found in terms of catalytic activity between zirconium oxide catalysts and Zr-SBA-15 materials can be attributed to the differences on Zr available to catalyze the hydrogenation step is going to be higher for ZrO_2, independently on the investigated phase. More difficult to explain are the differences found between ZrO_2/Si-SBA-15 and Zr-SBA-15(10), whose Zr loadings, theoretically, is the same. Even if it is considered that the theoretical amount of zirconium added during the preparation of the Zr-SBA-15 materials is not completely incorporated into the materials framework, the differences found in terms of conversion never could correlate with the differences in metal loading.

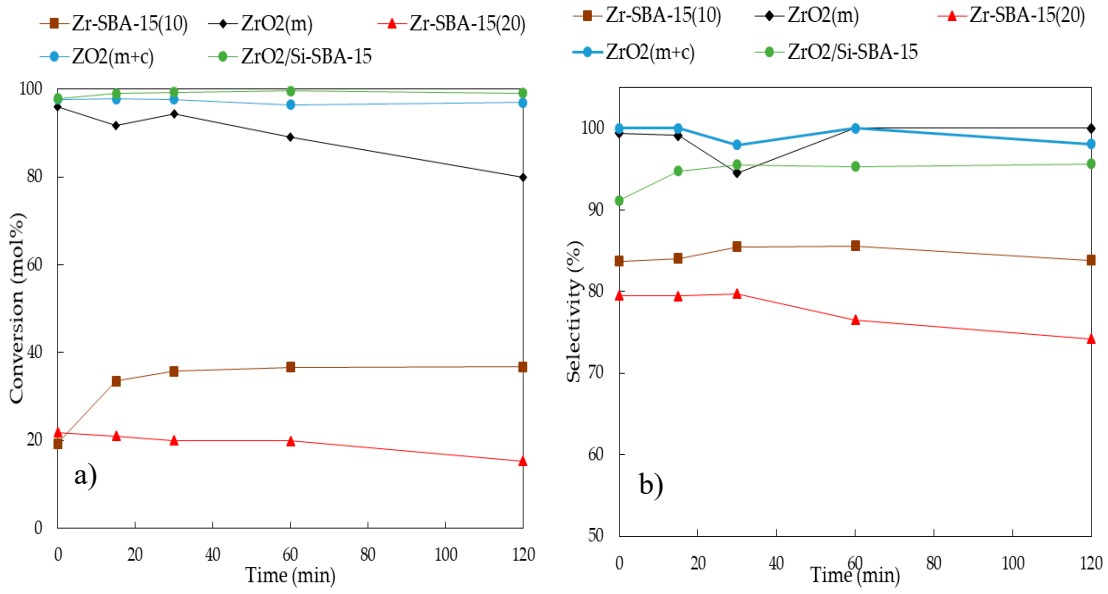

Figure 3. Catalytic activity of the Zr-based materials evaluated in the hydrogenation of ML to GVL expressed as: (**a**) conversion and (**b**) selectivity.

Apparently, ZrO_2 materials are the most effective materials in the conversion of ML to GVL with the highest selectivity towards the desired product. However, if the results are expressed as productivity it is possible to reach a better insight in terms of the efficiency of each material to boost the formation of GVL. Firstly, when Zr-SBA-15 materials are compared among them, the positive effect of increasing Zr content in the material framework is clear. Secondly, ZrO_2 catalyst showed

similar GVL productivity to that found for Zr-SBA-15(10). Thus, the better metal dispersion expected for Zr-SBA-15 materials as compared with bulk ZrO_2 is going to play an important role in the ML hydrogenation. Finally, the most remarkable result was found when it was compared the GVL productivity (mmol of GVL produced per hour and gram of catalyst) obtained by Zr-SBA-15(10) and ZrO_2/Si-SBA-15, both with the same synthesized with the same metal loading. The GVL productivity for ZrO_2/Si-SBA-15 was almost 3 times higher the value achieved by the other materials (Figure 4).

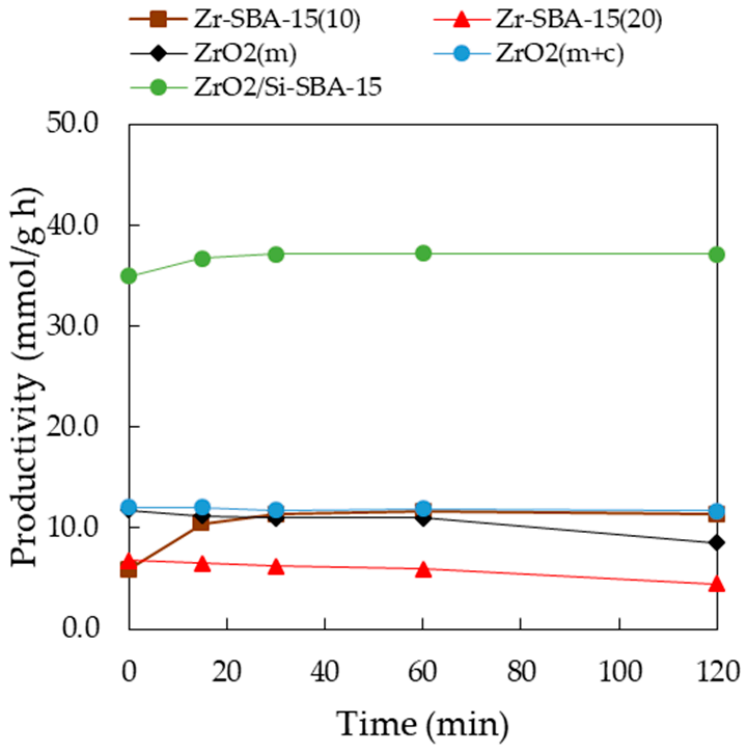

Figure 4. GVL Productivity obtained using the different zirconium materials investigated in the continuous ML hydrogenation. Reaction conditions: 0.1–0.2 g of catalyst, 0.2 mol/L ML in 2-propanol, flow rate: 2 mL/min, 30 bar, 200 °C followed during 2 h.

The differences found between Zr-SBA-15(10) and ZrO_2/Si-SBA-15 at first instance seem to be a bit contradictory. Nevertheless, Zr loading in both materials is not the only parameter that should be considered when compare the catalytic activity of both materials in the continuous ML hydrogenation. While in the material synthesized by wet impregnation (ZrO_2/Si-SBA-15) zirconium is expected to be in the external face of Si-SBA-15 channels and fully accessible by the reactant molecules, in Zr-SBA-15(10) catalyst, due to the nature of the material, an important fraction of Zr is going to be forming the walls.

Once selected the optimum catalyst for the transformation of ML to GVL over different Zr sites the influence of different experimental parameters was studied (Figure 5). Among them, pressure (10, 20 and 30 bar), temperature (120, 170, 200 bar) and flow rate (0.2, 0.5, 1 mL/min) were evaluated leaving constant the concentration of ML in 2-propanol. Firstly, the influence of temperature in the continuous hydrogenation of ML to GVL was investigated keeping constant the remaining reaction conditions (0.3 M methyl levulinate solution in 2-propanol, 0.2 mL/min flow rate, 30 bar pressure). At low temperature, 120 °C, any formation of GVL was detected while the minimum ML conversion was attributed to the transesterification of ML to produce isopropyl levulinate. Such transesterification reaction remained still important at higher temperature, 170 °C, where GVL becomes the main reaction product. A new increase in the reaction temperature impact positively in the selectivity towards GVL that is increased 95% when the reaction was performed at 200 °C as compared with the GVL selectivity obtained for the reaction at 170 °C that was 73%. Following the pressure effect was evaluated at three different pressure values (10, 20, 30 bar) controlling reaction temperature at 200 °C, 0.3 M solution

of ML was introduced in the system with a speed of 0.2 mL/min. The maximum GVL productivity was achieved when a pressure of 30 bar was used as compared with the other two pressures explored. While diminishing the pressure at 20 bar leads to a slight decrease in ML conversion and GVL selectivity, a further decrease at 10 bar leads to a lower GVL productivity and increased formation of the transesterification product, isopropyl levulinate. Pressure values below 10 bar lead to low values of GVL selectivity as well as ML conversion obtaining isopropyl levulinate as main product [23]. Thus, keeping relatively high it is possible to favor the hydrogenation pathway over ML transesterification with the solvent 2-propanol. Finally, the influence of ML 0.3 M solution flow rate was evaluated at 200 °C and 30 bars. Figure 5c clearly shows that an increase on the flow rate affects ML conversion negatively, while selectivity towards GVL remained high. Thus, to achieve a good GVL productivity, for ZrO_2/Si-SBA-15, it is necessary to keep the flow rate low at 0.2 mL/min.

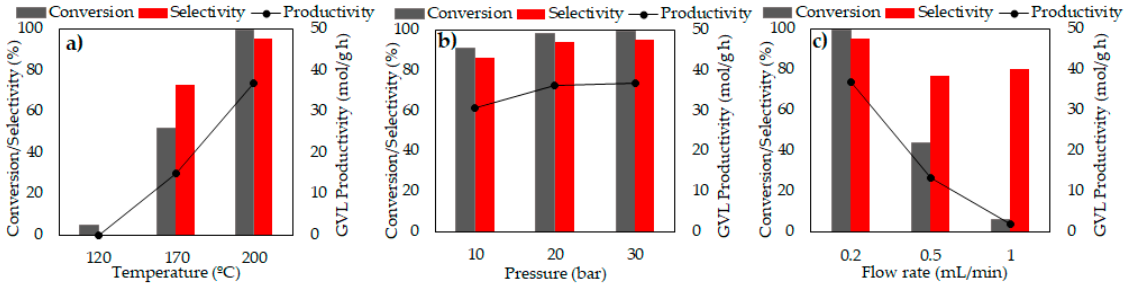

Figure 5. Catalytic performance of ZrO_2/Si-SBA-15 in the liquid-phase continuous transformation of ML into GVL under different reaction conditions: (**a**) temperature, (**b**) pressure, (**c**) ML solution flow rate. Reaction conditions: 0.3 M ML solution, 0.1 g of catalyst were fixed for all the experiments, (**a**) 0.2 mL/min flow rate, 30 bar pressure; (**b**) 0.2 mL/min flow rate and 200 °C reaction temperature and finally, (**c**) 30 bar pressure and 200 °C reaction temperature. Time on stream 1 h.

Additionally, a long-term test of ZrO_2/Si-SBA-15 for 24 h was carried out to test the catalyst stability (Figure 6). At low times on stream, below one hour, it is observed an induction period before achieving the maximum productivity. After 10 h on stream the performance of the catalyst decreased a minimal amount and then remained practically constant as proof of the stability of the catalyst under investigated conditions.

The results obtained in this research work were compared with other already published in literature, leaving room for improvement if compared with GVL productivity achieved by UiO-66 (92.3 mmol/g h) [23]. On the other hand, long-term experiments of the best material studied in this work showed a better stability with the time of ZrO_2/Si-SBA-15 as compared with UiO-66. Similar results were found by Rao et al. [31] who prepared several ZrO_2/Si-SBA-15 materials with different metal loadings using a higher amount of catalyst and harsher conditions (250 °C). Other Zr-based materials such as $Zr(OH)_4$ were evaluated in the hydrogenation of levulinate ester with poorer selectivity towards GVL (84.5%) as compared with the results herein obtained [32].

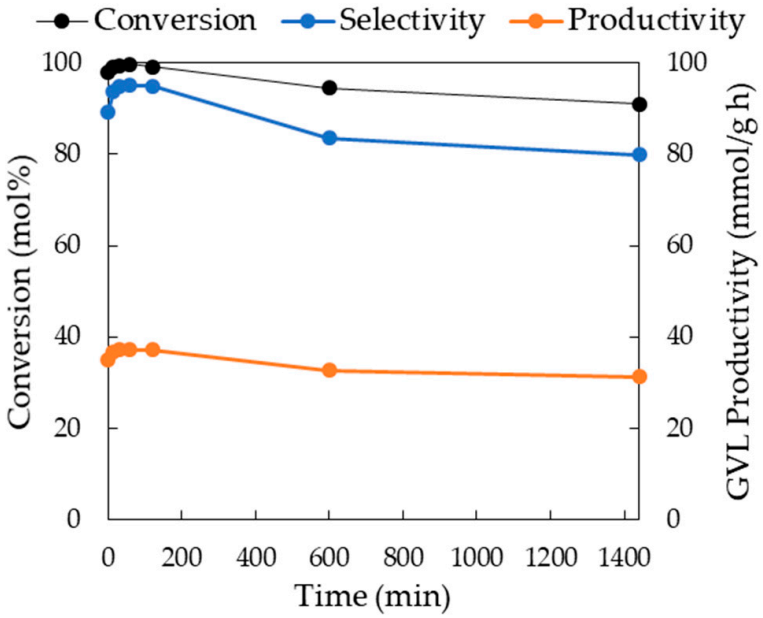

Figure 6. Long-term evaluation of ZrO_2/Si-SBA-15 catalytic performance in the continuous transformation of methyl levulinate into ϒ-valerolactone. Reaction conditions: 0.3 M ML solution, 0.1 g of catalyst, 0.2 mL/min flow rate, 30 bar, 200 °C. Time on stream up to 24 h.

3. Materials and Methods

3.1. Materials Preparation

3.1.1. Synthesis of Zr-SBA-15 Materials

Zr-modified SBA-15 materials were synthesized according to a protocol already described by our research group [17], using $ZrO(NO_3)_2{\cdot}xH_2O$ (Sigma-Aldrich, St. Louis, MI, USA) as metal salt precursor. For the preparation of Zr-SBA-15 materials with Si/Zr molar ratio of 20 and 10, 8 g of copolymer triblock $PEO_{20}PPO_{70}PEO_{20}$, known as Pluronic P123, (Sigma-Aldrich, St. Louis, MI, USA), used as surfactant, were dissolved in 300 mL HCl solution (pH ≈ 1.5) in a Teflon bottle. After approximately 2 h, 18 mL of tetraethyl orthosilicate (Sigma-Aldrich, St. Louis, MI, USA), used as silicon source, followed by the addition of the appropriate amount of the Zr precursor to achieve the previously mentioned molar ratios. The mixture is kept under stirring for 24 h at 35 °C and, subsequently, underwent hydrothermal treatment for 24 h. Once concluded the previous step, a white solid is formed and separated by filtration. The final zirconium silicates were obtained after calcining at 600 °C for 8 h and named as Zr-SBA-15(10) and Zr-SBA-15(20), where the numbers in brackets are the Si/Zr ratio in the synthesized materials.

3.1.2. Synthesis of Supported ZrO_2/Si-SBA-15

Same amount of Zr salt precursor as the used for the preparation of Zr-SBA-15(10) material was dissolved in 3 mL of distilled water and then 1 g of Si-SBA-15 was added to the zirconium containing solution. The mixture was stirred for 30 min and subsequently the water was removed using a rotary evaporator (Heidolph Laborota 4000, Schwabach, Germany). The dried solid obtained was calcined at 400 °C during 4 h with a heating rate of 2 °C/min.

3.1.3. Synthesis of ZrO_2

Two ZrO_2 oxides were synthesized at different pH values. Both were prepared following the same protocol described in Section 3.1. without adding TEOS. The samples were calcined at 600 °C

for 8 h and named ZrO_2(m) and ZrO_2(m+c), where m stands for monoclinic and m+c for monoclinic and cubic.

3.2. Materials Characterization

The nitrogen adsorption/desorption isotherm have been obtained at liquid nitrogen temperature (77K) using a Micromeritics ASAP 2000 porosimeter (Micromeritics Instrument Corp., Norcross, GA, USA). The amount of sample employed for each analysis was in a range 0.18–0.23 g, and prior to the analysis all the solids were outgassed at 130 °C for 24 h. The specific surface area of the synthesized materials has been calculated using the linear part ($0.05 < Po < 0.22$) of Brunauer, Emmett and Teller (BET) equation. Pore size distribution have been calculated using the adsorption branch and the Barrett, Joyner, and Halenda (BJH) equation (Barret-Joyner-Halenda). Pore volume have been calculated using the BJH formula.

The crystallinity and the structure of the synthesized catalysts have been evaluated using the X-ray diffraction technique. X-ray diffractograms were acquired using a Bruker D8D Discover (40 kV, 40 mA) diffractometer (Bruker AXS, Karlsruhe, Germany) using the Cu Kα radiation (λ = 1.54 Å). The scan speed was 0.5 or 1 °/min in the interval $0.5° < 2\theta < 5°$ for the low angle measurements and $10° < 2\theta < 80°$ for the wide-angle acquisitions. This is instrument is fitted with the "Diffract.Suite EVA" software version 3.1 (Bruker AXS, Karlsruhe, Germany) which allows particle size measurement and phase ratio determination.

Elemental analysis of the synthesized materials was carried out using a JEOL JSM 7800F scanning electron microscope (JEOL Ltd., Akishima, Tokio, Japón) fitted with a X-max150 microanalysis system, window type detector SiLi, detection range: from boron to uranium, 127 eV resolution at 5.9 KeV.

The surface acid properties were evaluated using a chromatographic pulse method using pyridine, which measures total acidity, and 2,6-dimethyl pyridine that interact, mainly, with the Brönsted acid sites. Lewis acidity was obtained by difference between total and Brönsted acidity. The measurements were carried out a gas chromatograph fit with a flame ionization detector (FID) detector and a Chromosorb AW-MCS 80/100 packed column of 0.5 m length containing 5% wt. % in polyphenylether (Supelco Analytical, Bellefonte, PA, USA). The operational conditions for the analysis were set up as follows: inlet temperature 300 °C, FID detector at 250 °C, and oven temperature was stablished at 70 °C and 90 °C for pyridine and 2,6-dimethyl pyridine, respectively.

Additionally, the qualitative evaluation of the acidity has been analyzed using DRIFT of adsorbed pyridine in the region between 1700 and 1400 cm^{-1}. The spectra were recorded at 100, 150, 200 and 300 °C to assess the acidity strength. The vibration modes at 1545 cm^{-1} corresponds with the interaction of the pyridinium cation with Brönsted acid sites, while at ca. 1442 cm^{-1} rise the band corresponding with Lewis acid sites. An ABB 3000 instrument provided with a PIKE Technologies DiffusIR (PIKE Technologies, Madison, WI, USA), a diffuse reflection accessory that can operate at different temperatures and gas environments.

3.3. Catalytic Activity

The catalytic activity of the synthesized materials was investigated in the ML hydrogenation using 2-propanol as hydrogen donor solvent. The amount of catalyst used was approximately 0.1 g, (0.1 g for SBA-15 materials and 0.2 g for ZrO_2 catalysts, based on material density). The optimum conditions to perform this reaction were stablished at 200 °C, at 30 bar pressure, with a 0.2 mL/min flow of a 0.3 M ML solution in 2-propanol. Additionally, different pressure, temperature, and ML solution flow were evaluated to determine the best reaction conditions to perform this reaction under continuous flow. Alicquots were collected one hour after the steady state conditions were reached in the reactor to ensure that the entire line was filled with ML solution.

The samples were analyzed in a series II Agilent 5890 GC, provided with a SUPELCO EQUITY TM-1 (60 m × 0.25 mm × 0.25 μm) column and an FID detector (Supelco Analytical, Bellefonte, PA, USA). The temperature in the injector as well as in the reactor were 250 °C. The oven temperature

program used was from an initial temperature of 60 °C for one minute that was increases up to 230 °C with a heating rate of 10 °C/min and remained constant at that temperature for 5 min. Reaction products were confirmed using a 7820A GC coupled with a 5977B mass spectrometer detector (Agilent Technologies, Santa Clara, CA, USA) using same analysis conditions as above.

4. Conclusions

Several materials based on zirconium: two SBA-15 zirconium silicates with two different Si/Zr molar ratio, two bulky ZrO_2 with different phases and ZrO_2 loaded on Si-SBA-15 (ZrO_2/Si-SBA-15) were investigated in the continuous ML hydrogenation to GVL using 2-propanol as hydrogen donor solvent. Among them, ZrO_2/Si-SBA-15 showed the best performance in terms of GVL productivity, which can be explained by, firstly by the better dispersion of the ZrO_2 particles as compared with the bulky oxides in addition to an expected lower particle size and, secondly, the better accessibility of the Zr sites in this material compared with the material Zr-SBA-15(10), with same Zr loading, where the zirconium sites is going to be in the material framework forming the SBA-15 walls. In addition, ZrO_2/Si-SBA-15 have displayed a significant stability with time on stream keeping almost constant GVL productivity with a slight decrease in selectivity and ML conversion. Also, it is noteworthy the high selectivity towards GVL achieved by all the investigated materials, with a minimal amount found of isopropyl levulinate, the transesterification product. Finally, the influence of several experimental variable on the continuous hydrogenation of ML by ZrO_2/Si-SBA-15 such as reaction temperature, system pressure and methyl levulinate solution feeding have been investigated. It was observed that high pressure and temperature affects GVL productivity positively while flow rates higher to 0.2 mL/min were too fast to convert ML efficiently.

Supplementary Materials: The following are available online at http://www.mdpi.com/2073-4344/9/2/142/s1, Figure S1: Nitrogen adsorption-desorption plots for the materials: (**a**) Zr-SBA-15(10), (**b**) ZrO2/Si-SBA-15, (**c**) Zr-SBA-15(20), (**d**) ZrO2(m). Figure S2: Low-angle XRD for selected materials: ZrO_2/Si-SBA-15, Zr-SBA-15(10), ZrO_2(m). Characteristics diffraction lines (100), (110), (200) corresponding with hexagonal arrangement are shown for SBA-15 materials.

Author Contributions: Conceptualization, R.L. and A.A.R.; methodology, A.P., A.A.R. and R.L.; investigation, N.L., A.F, W.O.; resources, A.P., A.A.R.; data curation, N.L., A.F, W.O.; writing—original draft preparation, A.P.; writing—review and editing, R.L., A.M.B.; visualization, A.P.; supervision, R.L., A.M.B., A.A.R; project administration, A.A.R, A.M.B.; funding acquisition, R.L.

Funding: This research was funded by RUDN University Program 5-100.

Acknowledgments: Antonio Pineda acknowledges the support of "Plan Propio de Investigación" from Universidad de Córdoba (Spain) and "Programa Operativo" FEDER funds from Junta de Andalucía. R.L. gratefully acknowledges funding from MINECO under project CTQ2016-78289-P, co-financed with FEDER funds, also for an FPI contract for A.F. (BES-2017-081560) under the framework of the granted project. The publication has been prepared with support from RUDN University Program 5-100.

Conflicts of Interest: The authors declare no conflict of interest.

References

1. Chheda, J.N.; Huber, G.W.; Dumesic, J.A. Liquid-Phase Catalytic Processing of Biomass-Derived Oxygenated Hydrocarbons to Fuels and Chemicals. *Angew. Chem. Int. Ed.* **2007**, *46*, 7164–7183. [CrossRef] [PubMed]
2. Climent, M.J.; Corma, A.; Iborra, S. Conversion of biomass platform molecules into fuel additives and liquid hydrocarbon fuels. *Green Chem.* **2014**, *16*, 516–547. [CrossRef]
3. Corma, A.; Iborra, S.; Velty, A. Chemical Routes for the Transformation of Biomass into Chemicals. *Chem. Rev.* **2007**, *107*, 2411–2502. [CrossRef] [PubMed]
4. Serrano-Ruiz, J.C.; Luque, R.; Sepulveda-Escribano, A. Transformations of biomass-derived platform molecules: From high added-value chemicals to fuels via aqueous-phase processing. *Chem. Soc. Rev.* **2011**, *40*, 5266–5281. [CrossRef] [PubMed]

5. Mehdi, H.; Fábos, V.; Tuba, R.; Bodor, A.; Mika, L.T.; Horváth, I.T. Integration of Homogeneous and Heterogeneous Catalytic Processes for a Multi-step Conversion of Biomass: From Sucrose to Levulinic Acid, γ-Valerolactone, 1,4-Pentanediol, 2-Methyl-tetrahydrofuran, and Alkanes. *Top. Catal.* **2008**, *48*, 49–54. [CrossRef]
6. Osakada, K.; Ikariya, T.; Yoshikawa, S. Preparation and properties of hydride triphenyl-phosphine ruthenium complexes with 3-formyl (or acyl) propionate [RuH(OCOCHRCHRCOR′)(PPh3)3] (R=H, CH3, C2H5; R=H, CH3, C6H5) and with 2-formyl (or acyl) benzoate [RuH(o-OCCOC6H4COR′)(PPh3)3] (R′=H, CH3). *J. Organomet. Chem.* **1982**, *231*, 79–90. [CrossRef]
7. Braca, G.; Maria, A.; Galletti, R.; Sbrana, G. Anionic ruthenium iodorcarbonyl complexes as selective dehydroxylation catalysts in aqueous solution. *J. Organomet. Chem.* **1991**, *417*, 41–49. [CrossRef]
8. Hengne, A.M.; Biradar, N.S.; Rode, C.V. Surface Species of Supported Ruthenium Catalysts in Selective Hydrogenation of Levulinic Esters for Bio-Refinery Application. *Catal. Lett.* **2012**, *142*, 779–787. [CrossRef]
9. Tan, J.J.; Cui, J.L.; Deng, T.S.; Cui, X.J.; Ding, G.Q.; Zhu, Y.L.; Li, Y.W. Water-Promoted Hydrogenation of Levulinic Acid to γ-Valerolactone on Supported Ruthenium Catalyst. *ChemCatChem* **2015**, *7*, 508–512. [CrossRef]
10. Kuwahara, Y.; Kaburagi, W.; Fujitani, T. Catalytic transfer hydrogenation of levulinate esters to γ-valerolactone over supported ruthenium hydroxide catalysts. *RSC Adv.* **2015**, 45848–45855. [CrossRef]
11. Vu, H.; Harth, F.M.; Wilde, N. Silylated Zeolites with Enhanced Hydrothermal Stability for the Aqueous-Phase Hydrogenation of Levulinic Acid to γ-Valerolactone. *Front. Chem.* **2018**, *143*. [CrossRef] [PubMed]
12. Wang, A.Q.; Lu, Y.R.; Yi, Z.X.; Ejaz, A.; Hu, K.; Zhang, L.; Yan, K. Selective Production of γ-Valerolactone and Valeric Acid in One-Pot Bifunctional Metal Catalysts. *ChemistrySelect* **2018**, *3*, 1097–1101. [CrossRef]
13. Gilkey, J.G.; Xu, B. Heterogeneous Catalytic Transfer Hydrogenation as an Effective Pathway in Biomass Upgrading. *ACS Catal.* **2016**, *6*, 1420–1436. [CrossRef]
14. Luo, H.Y.; Consoli, D.F.; Gunther, W.R.; Román-Leshkov, Y. Investigation of the reaction kinetics of isolated Lewis acid sites in Beta zeolites for the Meerwein–Ponndorf–Verley reduction of methyl levulinate to γ-valerolactone. *J. Catal.* **2014**, *320*, 198–207. [CrossRef]
15. Tang, X.; Hu, L.; Sun, Y.; Zhao, G.; Hao, W.W.; Lin, L. Conversion of biomass-derived ethyl levulinate into γ-valerolactone via hydrogen transfer from supercritical ethanol over a ZrO_2 catalyst. *RSC Adv.* **2013**, *3*, 10277–10284. [CrossRef]
16. Chia, M.; Dumesic, J.A. Liquid-phase catalytic transfer hydrogenation and cyclization of levulinic acid and its esters to γ-valerolactone over metal oxide catalysts. *Chem. Commun.* **2011**, *47*, 12233–12235. [CrossRef] [PubMed]
17. Gracia, M.D.; Balu, A.M.; Campelo, J.M.; Luque, R.; Marinas, J.M.; Romero, A.A. Evidences of the in situ generation of highly active Lewis acid species on Zr-SBA-15. *Appl. Catal. A* **2009**, *371*, 85–91. [CrossRef]
18. Wolf, P.; Hammond, C.; Conrad, S.; Hermans, I. Post-synthetic preparation of Sn-, Ti- and Zr-beta: A facile route to water tolerant, highly active Lewis acidic zeolites. *Dalton Trans.* **2014**, *43*, 4514–4519. [CrossRef]
19. Chareonlimkun, A.; Champreda, V.; Shotipruk, A.; Laosiripojana, N. Catalytic conversion of sugarcane bagasse, rice husk and corncob in the presence of TiO_2, ZrO_2 and mixed-oxide TiO_2-ZrO_2 under hot compressed water (HCW) condition. *Bioresour. Technol.* **2010**, *101*, 4179–4186. [CrossRef] [PubMed]
20. Pichler, C.M.; Al-Shaal, M.G.; Gu, D.; Joshi, H.; Ciptonugroho, W.; Schüth, F. Ruthenium Supported on High-Surface-Area Zirconia as an Efficient Catalyst for the Base-Free Oxidation of 5-Hydroxymethylfurfural to 2,5-Furandicarboxylic Acid. *ChemSusChem* **2018**, *11*, 2083–2090. [CrossRef]
21. Wattanapaphawonga, P.; Reubroycharoen, P.; Yamaguchi, A. Conversion of cellulose into lactic acid using zirconium oxide catalysts. *RSC Adv.* **2017**, *7*, 18561–18568. [CrossRef]
22. Garcia-Olmo, A.J.; Yepez, A.; Balu, A.M.; Prinsen, P.; Garcia, A.; Maziere, A.; Len, C.; Luque, R. Activity of continuous flow synthesized Pd-based nanocatalysts in the flow hydroconversion of furfural. *Tetrahedron* **2017**, *73*, 5599–5604. [CrossRef]
23. Ouyang, W.; Zhao, D.; Wang, Y.; Balu, A.M.; Len, C.; Luque, R. Continuous Flow Conversion of Biomass-Derived Methyl Levulinate into γ-Valerolactone Using Functional Metal Organic Frameworks. *ACS Sustain. Chem. Eng.* **2018**, *6*, 6746–6752. [CrossRef]
24. Fu, J.; Sheng, D.; Lu, X. Hydrogenation of Levulinic Acid over Nickel Catalysts Supported on Aluminum Oxide to Prepare γ-Valerolactone. *Catalysts* **2016**, *6*, 6. [CrossRef]

25. Bai, Y.; Cherkasov, N.; Huband, S.; Walker, D.; Walton, R.; Rebrov, E. Highly Selective Continuous Flow Hydrogenation of Cinnamaldehyde to Cinnamyl Alcohol in a Pt/SiO_2 Coated Tube Reactor. *Catalysts* **2018**, *8*, 58. [CrossRef]
26. Cherkasov, N.; Bai, Y.; Rebrov, E. Process Intensification of Alkynol Semihydrogenation in a Tube Reactor Coated with a Pd/ZnO Catalyst. *Catalysts* **2017**, *7*, 358. [CrossRef]
27. Huang, C.; Chen, S.; Fei, X.; Liu, D.; Zhang, Y. Catalytic Hydrogenation of CO_2 to Methanol: Study of Synergistic Effect on Adsorption Properties of CO_2 and H_2 in $CuO/ZnO/ZrO_2$ System. *Catalysts* **2015**, *5*, 1846–1861. [CrossRef]
28. Schüth, F.; Wingen, A.; Sauer, J. Oxide Loaded Ordered Mesoporous Oxides for Catalytic Applications. *Micropor. Mesopor. Mater.* **2001**, *44–45*, 465–476. [CrossRef]
29. Li, H.; Fang, Z.; Yang, S. Direct Conversion of Sugars and Ethyl Levulinate into γ-Valerolactone with Superparamagnetic Acid–Base Bifunctional ZrFeOx Nanocatalysts. *ACS Sustain. Chem. Eng.* **2016**, *4*, 236–246. [CrossRef]
30. Hernández, B.; Iglesias, J.; Morales, G.; Paniagua, M.; López-Aguado, C.; García Fierro, J.L.; Wolf, P.; Hermans, I.; Melero, J.A. One-pot cascade transformation of xylose into γ-valerolactone (GVL) over bifunctional Brønsted–Lewis Zr–Al-beta zeolite. *Green Chem.* **2016**, *18*, 5777–5781. [CrossRef]
31. Enumula, S.S.; Gurram, V.R.B.; Kondeboina, M.; Burri, D.R.; Kamaraju, S.R.R. ZrO_2/SBA-15 as an efficient catalyst for the production of γ-valerolactone from biomass-derived levulinic acid in the vapour phase at atmospheric pressure. *RSC Adv.* **2016**, *6*, 20230–20239. [CrossRef]
32. Tang, X.; Chen, H.; Hu, L.; Hao, W.; Sun, Y.; Zeng, X.; Lin, L.; Liu, S. Conversion of biomass to γ-valerolactone by catalytic transfer hydrogenation of ethyl levulinate over metal hydroxides. *Appl. Catal. B* **2014**, *147*, 827–834. [CrossRef]